Study of the annealing influence on the mechanical performance of PA12 and PA12 fibre reinforced FFF printed specimens

Isaac Ferreira
Department of Mechanical Engineering, Faculdade de Engenharia da Universidade do Porto, Porto, Portugal and Department of Mechanical Engineering, Instituto Nacional de Estadística y Geografía, Porto, Portugal

Carolina Melo
Department of Mechanical Engineering, Faculdade de Engenharia da Universidade do Porto, Portugal

Rui Neto
Department of Mechanical Engineering, Faculdade de Engenharia da Universidade do Porto, Porto, Portugal and INEGI – Instituto de Ciência e Inovação em Engenharia Mecânica e Engenharia Industria, Porto, Portugal

Margarida Machado
IINEGI – Instituto de Ciência e Inovação em Engenharia Mecânica e Engenharia Industria, Porto, Portugal

Jorge Lino Alves
Department of Mechanical Engineering, Faculdade de Engenharia da Universidade do Porto, Porto, Portugal, and

Sacha Mould
Digital Transformation COLAB – DTx, Campus de Azurém, Guimarães, Portugal

Abstract

Purpose – The purpose of this study is to evaluate and compare the mechanical performance of FFF parts when subjected to post processing thermal treatment. Therefore, a study of the annealing treatment influence on the mechanical properties was performed. For this, two different types of Nylon (PA12) were used, FX256 and CF15, being the second a short fibre reinforcement version of the first one.

Design/methodology/approach – In this study, tensile and flexural properties of specimens produced via FFF were determined after being annealed at temperatures of 135°C, 150°C or 165°C during 3, 6, 12 or 18 h and compared with the non-treated conditions. Differential scanning calorimetry (DSC) was performed to determine the degree of crystallinity. To evaluate the annealing parameters' influence on the mechanical properties, a full factorial design of experiments was developed, followed by an analysis of variance, as well as post hoc comparisons, to determine the most significative intervening factors and their effect on the results.

Findings – The results indicate that CF15 increased its tensile modulus, strength, flexural modulus and flexural strength around 11%, while FX256 presented similar values for tensile properties, doubling for flexural results. Flexural strain presented an improvement, indicating an increased interlayer behaviour. Concerning to the DSC analysis, an increase in the degree of crystallinity for all the annealed parts.

Originality/value – Overall, the annealing treatment process cause a significant improvement in the mechanical performance of the material, with the exception of 165°C annealed specimens, in which a decrease of the mechanical properties was observed, resultant of material degradation.

Keywords Additive manufacturing, Composite materials, Annealing, DOE, FFF, PA12, Composites, Short fibre

Paper type Research paper

1. Introduction

In an era of progress and innovation, the incessant demand for continuous improvement of the current technologies, as well as the introduction of new ones are a reality. Additive manufacturing (AM) is already well established as a production method; however, the evolution and demand for better parts is continuously pushing the barrier on these processes and material properties (Wohlers, 2018). According to ISO/ASTM 52900 (2015), there are seven AM groups based on the different types of processing and materials, which comprise

The current issue and full text archive of this journal is available on Emerald Insight at: **https://www.emerald.com/insight/1355-2546.htm**

Rapid Prototyping Journal
26/10 (2020) 1761–1770

[DOI 10.1108/RPJ-10-2019-0278]

Author gratefully acknowledge the funding of Project POCI-0145-FEDER-016414-FIBR3D-Additive manufacturing based on hybrid processes for long or continuous fibre reinforced polymeric matrix composites, co-financed by Programa Operacional Regional de Lisboa (LISBOA 2020) and by the Project NORTE-01-0145-FEDER-000022-SciTech, cofinanced by NORTE2020, through FEDER.

Received 28 October 2019
Revised 6 January 2020
4 May 2020
Accepted 11 August 2020

Rapid Prototyping Journal
Volume 26 · Number 10 · 2020 · 1761–1770

polymers, composites (Fonseca et al., 2019; Liu et al., 2019), metals (Gibson et al., 2018), ceramics (Chen et al., 2019) and glass (Dong et al., 2019). Thus, with such an expressive growth of these technologies, it becomes important to analyse the possible post-processing techniques to improve the mechanical performance of the components produced by additive manufacturing. The FFF process is one of the most widely used additive manufacturing techniques, as it allows to produce highly flexible/customizable parts with complex geometries in a reduced period, at low cost, when compared to other polymer based AM techniques. FFF can process a wide range of materials, from the common use polylactic acid (PLA) to engineering polymers as polyamides (PA), high performance polymers such as polyether ether ketone (PEEK) and composites, granting a full spectrum of mechanical properties. As the level of complexity of the material increase, also processing temperatures and consequently the difficulty of the process. The successive heating and cooling cycles inherent to the process, create thermal residual stresses, leading to inadequate aesthetics and mechanical performance; thus, post-processing thermal treatment of annealing is recommended to solve this type of problems. Annealing is a type of thermal treatment used to improve mechanical performance and stability in materials. For polymers, annealing induces a micro structural recrystallization and reorganization of the amorphous phase in the material via temperature increase during a certain period of time above its glass transition point (T_g) (Bai et al., 2011; Gogolewski et al., 1980; Fischer, 1972).

To the best of the authors' knowledge, few studies have been conducted regarding thermal treatment influence on the mechanical performance of FFF printed parts (Dong et al., 2019; Rangisetty and Peel, 2017; Hart et al., 2018). Dong et al. (2019) analysed the influence of the annealing process on the flexural behaviour of polylactic acid (PLA) and PLA grafted cellulose nanofibres. Both types of specimens were thermally annealed above the glass transition temperature for a total of six temperature combinations. These specimens where then submitted to flexural testing showing that the unannealed specimens were partly damaged, while the thermally treated specimens preserved their structure enhancing the mechanical properties. Rangisetty and Peel (2017) studied the influence of the annealing process on tensile and flexural specimens, considering different infill patterns. Specimens were printed with commodity polymers such as PLA, acrylonitrile butadiene styrene (ABS) and polyethylene terephthalate glycol (PETG), along reinforced versions, even though provided by different feedstock producers. The specimens were annealed 5°C above the glass transition temperature during 1 h. The results present an increase in tensile strength for PLA and PET, sorting no effect on ABS. Young's modulus was also higher for PLA annealed specimens (only unreinforced specimens), while ABS presented a decrease in performance. Both PETG-based materials presented an increase in modulus. Flexural strength increases significantly for PLA and PETG, while flexural modulus shows an improvement for pure PLA, reinforced ABS and considerable decrease in both PETG materials. As a result of the distinct materials, from different manufacturers, even considering the same type of polymer, may be the reason for the discrepancy in the results. Hart et al. (2018) studied the improvement of the interlayer fracture toughness of specimens printed in ABS when annealed. Single edge notch bend fracture specimens were produced and submitted to several temperature/time conditions, however inserted in a specially developed aluminium fixture, which compresses the specimens during treatment. Results show an increase in fracture toughness of 2500%. Thermal treatments were also used as a method for testing the effect of thermal ageing on the impact damage resistance and flexural behaviour of carbon fibre-reinforced epoxy laminates (García-Moreno et al., 2019). For thermosetting matrix composites, it was found and improvement in the impact resistance and flexural behaviour, induced by enhancements in crosslink density, which occurred for thermal treatments below the glass transition temperature (T_g). For treatment temperatures around and above the T_g, a decrease in performance is shown. As the presented work focuses in thermoplastics, thermal ageing could also occur, however not in the same conditions.

In this work, the annealing of the same commercial unfilled PA 12 and short fibre-reinforced FFF printed parts is studied via full factorial design of experiences (DOE) along with ANOVA statistical analysis to analyse the influence of temperature and annealing time on tensile and flexural performance, thermal properties were also analysed. The aim is to understand the fibre influence on the part properties when submitted to the temperature cycle and compare it with the pure matrix material.

This work is structured as follows: an introductory Section 1 that sums up the state of the art of the annealing treatment in FFF printed parts; afterwards, the experimental procedure is described in detail in Section 2 by addressing the materials, production method, annealing DOE and statistical analysis. Following, the results are analysed in Section 3, and lastly conclusions are drawn in Section 4.

2. Experimental procedure

2.1 Materials

Two versions of a commercial Polyamide 12 (PA 12) of ø 1.75-mm feedstock were bought from Fillamentum ©, Parzlich s.r.o (Czech Republic) and used as a basis of this study. CF15 is reinforced with short carbon fibres (100 μm in length and 10 μm in diameter) with a content of 15 Wt.%, being that, FX256 is the unreinforced version of CF15. Some of the datasheet material specifications are presented in Table 1, in which some unexpected values are presented, such as higher tensile modulus for the unreinforced material.

2.2 Material conditioning

PA-based materials are highly hygroscopic; hence, controlling the moisture content is demanded as it affects the mechanical

Table 1 Datasheet material specifications

Property	CF15	FX256
Material density (g/cm^3)	1.08	1.01
Melt flow index (g/10 min)	9.92	95
Tensile strength (MPa)	54.50	45.00
Tensile modulus (MPa)	500	1400
Melting temperature (°C)	160	178
Print temperature (°C)	235–260	235–260

Source: Parzlich s.r.o. Fillamentum (2018, 2019) performance of 3-D printed parts, as has already been demonstrated by several scientific studies (Carrascal *et al.*, 2005; Rajeesh *et al.*, 2010; Do *et al.*, 2015). Thus, in both stages of printing and testing, the same material conditioning is required to non-compromise the mechanical properties. Extruding a non-dried out material through a nozzle will cause irregularities in the part surface, originated by vaporization of the moisture content. The materials were provided hermetically sealed with silica gel; however, after each printing day, both materials were dried in a PrintDry™ (Canada) filament drier at 70°C for 8 h. After being printed, each set of specimens was placed in a sealed bag with silica gel.

2.3 Preparation of the printed specimens

Due to the large amount of specimens needed for this study, two printing devices were used. FX256 specimen production was performed in a Tronxy X5 3D printer from Shenzen Tronxy Technology Co. Ltd equipped with a brass nozzle. The reinforced specimens, the were printed in a Ratrig V-Core from Ratrig (Portugal) equipped with a hardened A2 steel, which is demanded due to the abrasiveness of the fibres. Both machines used the same extruder configuration, the same heated bed surface and the same slicing configuration designed in Simplify3D® 4.1.1. Table 2 lists the parameters used in the production of the specimens. As printing 100% dense parts leads to high warping levels, extra (disposable) skirt outlines and glue were added to improve bed adhesion. The choice of the remaining parameters was based on preliminary tests, which revealed ideal for this type of specimens, leading to improved printability, warping minimization and a better visual appearance (Fonseca *et al.*, 2019).

2.4 Mechanical testing

Five tensile specimens were printed according to ISO 527–2 1 A (International Standards Organization, 2012) for each condition (Table 4), with the parameters mentioned in Table 2 in an INSTRON® 5900 R (Illinois Tool Works Inc. USA) at 1 mm/min speed and a 5 kN load cell. Five flexural specimens were produced (for each DOE condition) with same methodology and tested according to ISO 178 (International Standards Organization, 2010), in a TIRAtest 2705, Tira GmbH (Germany).

Table 2 Selected printing parameters

Nozzle diameter	0.4 mm
Nozzle material	brass/A2 steel
Layer height	0.3 mm
Number of perimeters per layer	2
Infill percentage	100%
Infill pattern	Rectilinear ±45
Skirt outlines	7
Extrusion temperature	260°C
Bed temperature	90°C
Bed surface	Tempered glass + CUBE® glue
Printing speeds	40 mm/s
Extrusion multiplier	1.04

2.5 Differential scanning calorimetry analysis and annealing conditions

2.5.1 Differential scanning calorimetry test

Differential scanning calorimetry (DSC) (200 F3, Netzsch GmbH, Germany) was conducted at a heating rate of 10°C/min under nitrogen purge. The specimens were obtained from 10 × 10 × 4 [mm^3] printed parts with weights in the range of 10–20 mg. The temperatures varied from 30°C to 220°C, being performed two heating cycles along with the cooling scanning. For analysis purposes, the first heating cycle was not represented as it was performed to eliminate any possible effects of thermal history. A specimen of each material was tested to define the temperature interval that the annealing process should be done. Posteriorly to the annealing process, a treated specimen of each temperature was also submitted to DSC testing to identify potential changes in the material thermal behaviour.

2.5.2 Annealing

The thermal treatment was performed in a POL-EKO Aparatura® SLW32 (Wodzislaw Slaski, Poland) drying oven, with a heating rate of 7°C/min and a cooling rate of 1°C/min. Thus, it is implied that higher annealing tests result in longer cooling time. Annealing temperatures were defined considering the DSC results (performed previously to untreated specimens) to avoid critical transition points. As demonstrated in Table 3, a test per specimen was performed, identical melting temperatures (T_m) are found in both polymers, while small differences are found for the other transition points; therefore, the same temperatures were used. A 10 to 15°C gap below (T_m) was considered, and three stages of temperature were selected as the test values (165°C, 150°C and 135°C) with a 15°C interval, going bellow the crystallization temperature (T_c). The annealing time was 3, 6, 12 and 18 h as presented in the experimental plan of Figure 1.

Table 3 FX256 and CF15 DSC results for the control specimens

Material	T_g [°C]	T_c [°C]	T_m [°C]	ΔH_f [J/g]	X[%]
FX256	44.7	143.2	176.3	35.5	16.9
CF15	52.9	150.4	178.5	14.9	6.10

Figure 1 Experimental plan

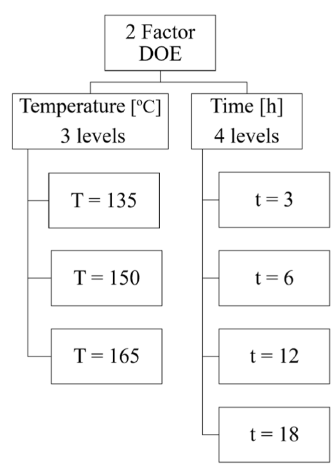

Rapid Prototyping Journal
Volume 26 · Number 10 · 2020 · 1761–1770

To calculate the crystallinity percentage (X[%]), the following equation was used (Canevarolo, 2002):

$$X[\%] = \frac{\Delta H_f}{\Delta H_f^*} \quad (1)$$

where ΔH_f is the material fusion enthalpy and ΔH^*_f is the fusion enthalpy of the 100% crystalline, values which can be found in literature (Blaine, 2002).

2.6 Design of experiments and analysis of variance

To better understand the results, a two factor (annealing temperature and time) full factorial DOE was developed where all the possible combinations were tested per material. For each condition, a specimen for thermal analysis test, five flexural, five tensile specimens per material were printed (beyond the non-treated specimens), then subjected to thermal treatment and consequent testing. Temperature, considered as the first factor, was tested for the three different levels, while the second factor (time) for four distinct time intervals were studied. The experimental data obtained from the mechanical tests was investigated via analysis of variance (ANOVA), to identify the truly contributive parameters considering a confidence interval of 95%. In addition to ANOVA, the main effect plots and interaction plots are presented, and as there are three and four response levels, post hoc Fisher least significant difference (LSD) pairwise comparisons (with a 95% confidence interval) were performed to the groups that presented p-value < 0.05 (except interactions), to identify for each response group, which is the best parameters combination. An alternative to Fisher LSD was Tukey HSD post hoc comparison method, which is a more rigorous method, however much harder to find the difference among results, and as a high number of tests was performed, the first method was preferred. This statistical analysis was performed with Minitab® 18. Table 4 depicts the full factorial DOE used for this test.

3. Results

3.1 Differential scanning calorimetry results

DSC analysis was performed in both polyamide materials, for one specimen of the three test temperatures, being chosen the 6 h time interval. Comparing the results for the control specimens presented in Table 3 with the Table 5, it is possible to observe an unexpected decrease in T_g of almost 10°C for both types of material, which might be justified by some degradation. T_c and T_m showed an increase, which is not considered significant. The increase in ΔH_f[J/g] is directly related with the X[%] values, as shown by equation (1). Table 5's last column presents the increase in crystallinity percentage facing the control specimens, in which FX256 is approximately of 100%, while the reinforced material presents an increase above 400%. It is also shown that, as the annealing temperature increases this percentage also grows, which can be explained by a longer cooling period, which allowed for the a better molecule organization. For the range of studied temperatures, non-significant differences are reported.

Table 4 Full factorial DOE and condition 0

Condition – C	Temperature – T [°C]	Time – t [h]
0	Control – Non-treated specimens	
1	135	3
2	135	6
3	135	12
4	135	18
5	150	3
6	150	6
7	150	12
8	150	18
9	165	3
10	165	6
11	165	12
12	165	18

3.2 Visual analysis

Colour alteration can be seen as a sign of property change of specimens, evidencing chemical ageing, as seen in previous works (Sang *et al.*, 2017). This analysis was not performed in the reinforced specimens due to the lack of transformation in its dark texture. Figures 2 and 3 depict a tensile and flexural specimens per annealing condition. Specimen C0 indicates the original colour of the non-treated specimens. Considering the temperatures and time interval at which the specimens were exposed (Table 4), at the lowest (C1-C4) and intermediate (C5-C8) temperature conditions the colour of the specimens evolved from white to light yellow and white to dark yellow, respectively, after increasing the exposure time. Furthermore, when using the highest temperature conditions (C9 to C12), yellowness becomes much more pronounced, going from light yellow to a dark brown. This change in colour is related to the oxidation of the PA resin (Sang *et al.*, 2017; Fan *et al.*, 2016). Through the specimen fracture it is possible to observe that this change in colour is not only on the outside but also throughout its core. The tensile control specimen C0 presented necking in the fracture area and a clear white colouration. From C1 until C6, overall elongation of the neck area is observed and an irregular fracture due to its ±45° pattern. From C7 onwards, it is possible to observe a slight elongation accompanied by fragile fracture perpendicular to the loading direction.

3.3 Mechanical properties

Figures 4 and 5 represent the tensile and flexural results, respectively. Figure 4(a) depicts the Young's modulus results,

Table 5 DSC results for annealed specimens t = 6h

Condition	T_g[°C]	T_c[°C]	T_m[°C]	ΔH_f[J/g]	X[%]	↑[%] X[%]
FX256						
T = 135°C	36.77	146.98	180.71	85.19	34.77	105.74
T = 150°C	37.66	146.79	181.07	86.51	35.31	108.94
T = 165°C	37.96	148.49	180.24	94.67	38.64	128.64
CF15						
T = 135°C	36.84	154.68	180.40	80.25	32.76	437.05
T = 150°C	39.81	154.62	180.47	81.55	33.29	445.74
T = 165°C	41.76	155.36	179.97	81.66	33.33	446.39

Rapid Prototyping Journal
Volume 26 · Number 10 · 2020 · 1761–1770

Figure 2 Tensile FX256 specimens after test for each annealing condition

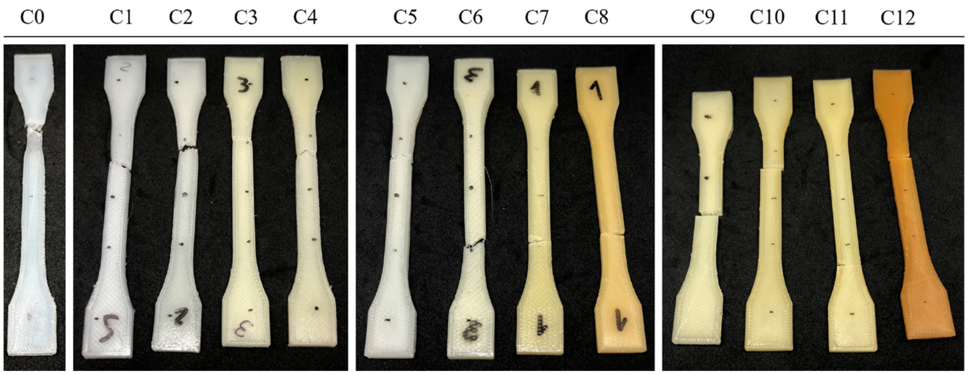

Figure 3 Flexural FX256 specimens after test for each annealing condition

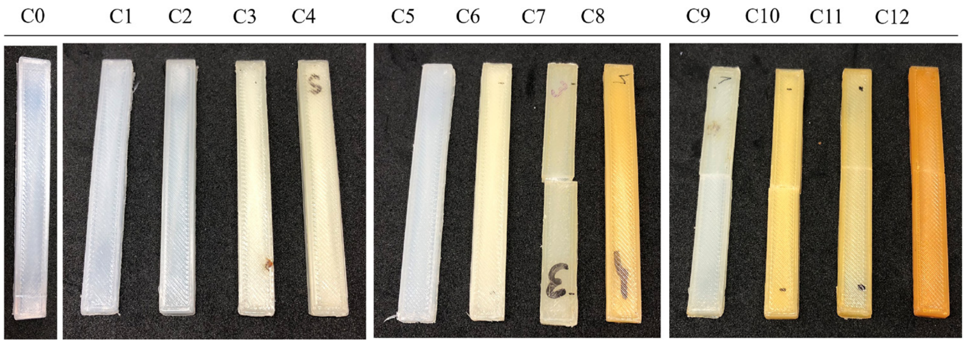

Figure 4 Tensile results comparisonNotes: (a) Young's modulus, (b) tensile strength and (c) strain at break

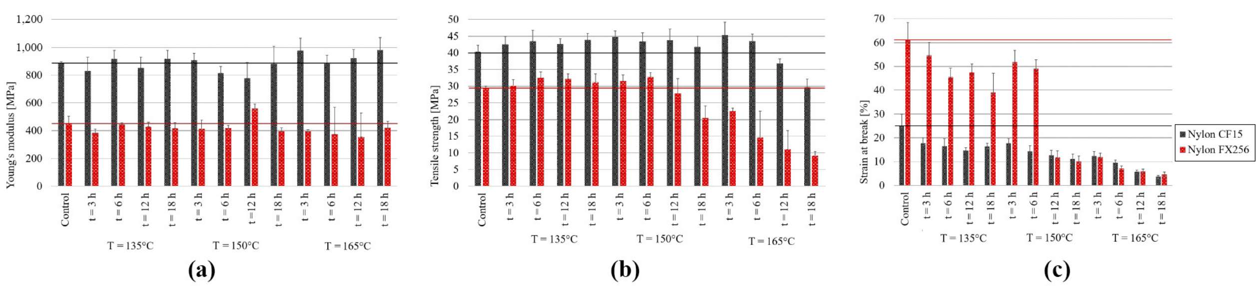

Notes: (a) Young's modulus; (b) tensile strength; (c) strain at break

Figure 5 Flexural results comparison

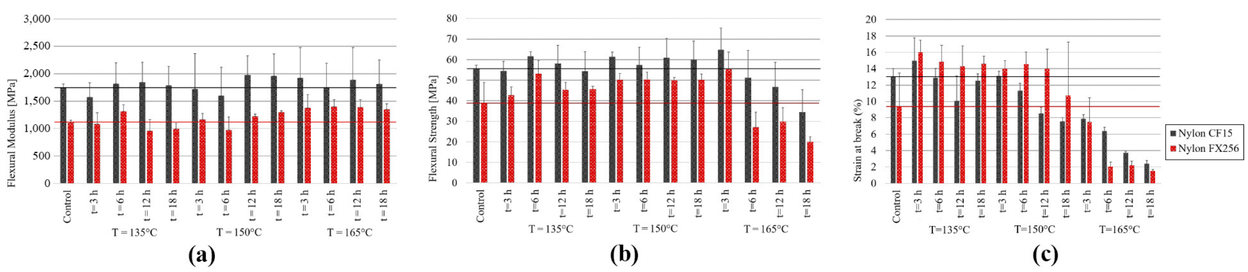

Notes: (a) Flexural modulus; (b) flexural strength; (c) flexural strain in which is possible to confirm that the reinforced parts present higher values than the unreinforced FX256. The CF15 control specimen indicates 886 MPa, while the treated specimens range from 780 to 980 MPa. FX256 results indicate a 450 MPa for the control and a range from 355 to 560 MPa. As for tensile strength 4b, the decrease is observed for higher temperatures for both materials, going from 45 to 30 MPa for the reinforced and 33 to 9 for the unreinforced is observed. Considering the strain at break, FX256, as expected, presents much higher values, until T = 150° C/t = 12h, changing from 51 to 5% mainly due to material degradation as seen previously in literature (Abhari *et al.*, 2017). The reinforced material shows a constant decrease along the test conditions, varying from 25 to 4%.

Flexural modulus [Figure 5(a)] that CF15 presents better results, ranging from 1500 to 2000 MPa, while FX256 presents values from 950 to 1400 MPa. In addition, it is notorious an increase in properties when facing the control specimen for both materials. Considering flexural strength (Figure 5b), CF15 values are in the interval of 35 to 64 MPa, while for FX256 is 20 to 55 MPa. It was found that higher temperatures tend to result in lower values of strength for both materials. Flexural strain [Figure 5(c)] results show once again that higher temperatures are worst for the mechanical performance, being more susceptible the unreinforced material, ranging from 1.5 to 16%, while CF15 varied from 2.4 to 15%.

3.4 Analysis of variance results

To better comprehend the results, with the purpose of finding the maximizing condition considering the type of property needed, an ANOVA analysis was performed for each result obtained via tensile and flexural result (Modulus, strength and strain at break). To simplify the data presentation, ANOVA results are depicted in APA style (F(degrees of freedom, remaining degrees)=F value, p = value).

3.4.1 CF15 – tensile

Through ANOVA analysis considering Young's modulus as a response, it is shown that only the temperature is statistically influential, with a contribution of 18.25% [F(2,48) = 6.70, p = 0.003]. Post hoc Fisher LSD method with a confidence level of 95% indicates that all T = 135/150°C have identical mean values, thus no significative difference between them. Through the main effect plot depicted in Figure 6, it is possible to verify that 165° C is the value that increases the most the modulus for this material.

For tensile strength, ANOVA shows that the T [F(2,48) = 13.95, $p < 0.001$] had a contribution of 16.42%, while t [F(3,48) = 12.07, $p < 0.001$], 21.31% and the interaction T-t [F(6,48) = 9.64, $p < 0.001$], a contribution of 34.03%, thus being the three influential groups. Post hoc Fisher LSD comparison shows that temperatures of 150/135°C have similar mean values and no significative difference between them, differentiating from 165°C. For t = 3 and 6 h, means are also statistically similar, whereas for 12 and 18 h present distinct mean results. This leads to conclude, according to the main effects plot of Figure 7 that higher strengths are obtained for the 135–150°C at 3–6 h intervals. The interaction plot show that throughout the selected time intervals, T = 135/150°C, modulus decreases slightly, while for T = 165°C, there is a significant decrease after 6 h.

Strain at break ANOVA results show that, T [F(2,48) = 94.93, $p < 0.001$] presented a contribution of 56.77% and t [F(3,48) = 21.05, $p < 0.001$] a contribution of 21.11%, while T-t interaction [F(6,48) = 13.51, p = 0.014] presented a contribution of 6.08%. Fisher LSD comparison shows that the three temperatures present significative different means, while for t = 12 and 18 h identical means are presented, consequently no significative difference between the two. Considering Figure 8 and the results obtained by the comparison method, it is possible to conclude that, the strain is maximized at T = 135° C, t = 3h. Interaction plot also shows that the general trend is the decrease in strain at break for higher treatment durations, being the worst results obtained for T = 165°C.

3.4.2 CF15 – flexural

ANOVA analysis to flexural modulus indicate that none of the variables are statistically influential since t, T and t-T $p > 0.05$, not being possible to reject the null hypotheses.

In what concerns flexural strength, ANOVA analysis show that T [F(2,48) = 5.79, p = 0.006] contributes of 13.76%, t [F(3,48) = 2.82, p = 0.049] with a contribution of 10.05%, while t-T interaction [F(6,48) = 2.69, p = 0.025] contributes 19.16%. Through Fisher LSD post hoc comparison it is possible to understand that for T = 150 and 135° C have identical statistical means resulting in no significative difference between the two. Using the same comparison for time group, it is possible to verify that 3/6/12 h have similar statistical means, while 6/12/18 h are also in other similar group, this means that 3 and 18 h are the only terms that do not present identical means,

Figure 6 CF15 – Young's modulus main effects plot

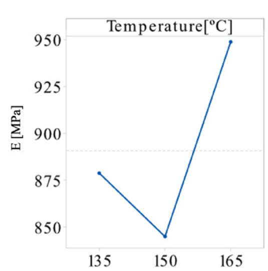

Figure 7 CF15 – Tensile strength main effects and interactions plots

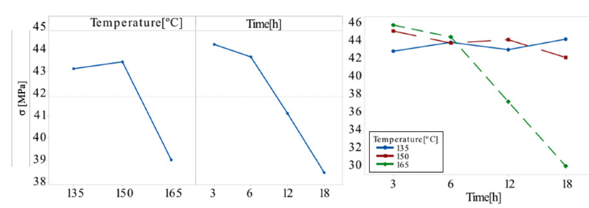

Figure 8 CF15 – Strain at break main effects and interactions plots

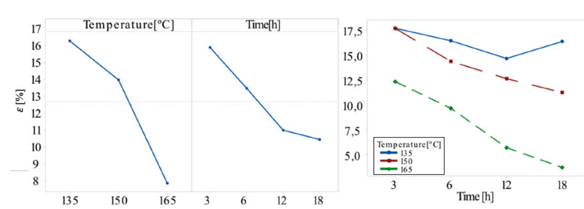

Rapid Prototyping Journal
Volume 26 · Number 10 · 2020 · 1761–1770

being statistically different. Main effect plots (Figure 9) present that higher flexural strain is obtained for T = 135/150° C, while for t = 3 is the best time interval for improved properties. Through the interactions plot, it is possible to observe that T = 165 shows a decrease in behaviour as the annealing time increases, while the other two temperatures oscillate with higher treatment time.

Flexural strain ANOVA analysis indicate that T [$F(2,48) = 115.03$, $p < 0.001$] contributes of 62.08%, while t [$F(3,48) = 28.84$, $p < 0.001$] contributes of 23.35%. As far as the interaction, was not considered statistically relevant since its p value was outside the confidence level of 95%. Given the Fisher LSD post hoc comparison it is possible to conclude that the three temperatures present distinct mean values, thus being all three statistically significant. As far as annealing time, only 18 and 12 h present identical means, therefore no significative difference between both is found. Figure 10 shows that the higher flexural strain is found for the combination 135°C/3 h.

3.4.3 FX256 – tensile

Through the ANOVA analysis to Young modulus, it was shown that none of the variables are statistically influential since t, T and T-t $p > 0.05$, not being possible to reject the null hypotheses at a confidence interval of 95%.

With regard to tensile strength, ANOVA shows that T [$F(2,48) = 106.57$, $p < 0.001$] contributes of 65.48%, while t [$F(3,48) = 11.49$, $p < 0.001$] with a contribution of 10.60%, while the interaction T-t [$F(6,48) = 4.97$, $p < 0.001$] gives a contribution of 9.17%. Taking into account Fisher comparison method, it is found that all three temperatures present statistically distinct means; therefore, all three must be considered. With regards to time values, 3 and 6 h present identical means, thereby no statistical evidences are shown that distinct one from the other. Through the main effect plot (Figure 11) taking into account the previous considerations that, the best behaviour is found at 135° C/3-6h. Interaction plot depicts that at T = 135 shows minimal change for different treatment times, while for T = 150°C, a decrease is observed after t = 6h. T = 165°C presents a shows a decreasing behaviour

Figure 9 CF15 – Flexural strength main effects and interactions plots

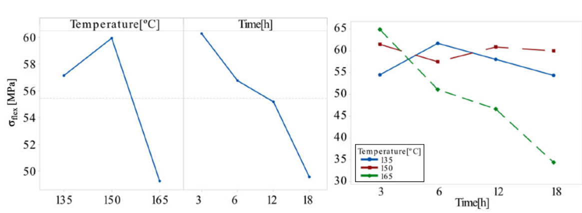

Figure 10 CF15 – Flexural strain main effects plots

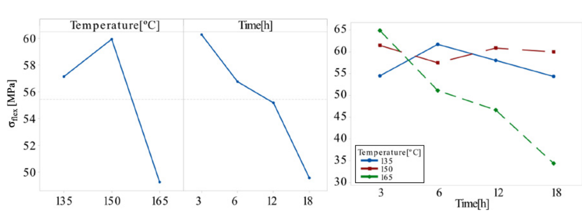

Figure 11 FX256 – Tensile strength main effects and interactions plots

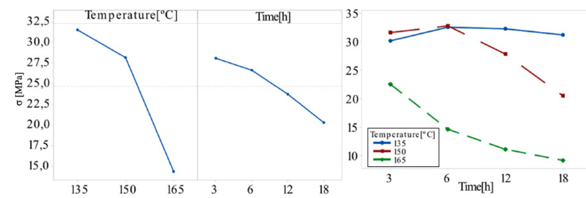

along the test time, being more pronounced at lower time intervals.

Considering the strain at break, ANOVA results indicate that T [$F(2,48) = 427.42$, $p < 0.001$] contributes of 62.28%, while t [$F(3,48) = 83.88$, $p < 0.001$] with a contribution of 18.33%, whereas the interaction T-t [$F(6,48) = 36.35$, $p < 0.001$] presents a contribution of 15.89%. Post hoc Fisher LSD showed that all temperature groups have distinct means, each one presenting relevant difference in the response. The same differences are found for all the time values. Main effect plot in Figure 12 shows that the improved performance is found at for 135°C/3h, whereas the combination plot shows a clear worst behaviour at T = 165°C along the time, for T = 135°C, a slight decrease along the time, while for T = 150°C above 6 h is found an abrupt decrease in strain at break.

3.4.4 FX256 – flexural

For flexural modulus, ANOVA results show that T [$F(2,48) = 15.55$, $p < 0.001$] contributes 30.49%, while t group does not fulfil the condition $p < 0.05$, thus not being considered for this set of results, whereas the interaction T-t [$F(6,48) = 3.76$, $p < 0.004$] presents a contribution of 22.09%. A comparison using Fisher LSD method shows that T = 135/150° C presents similar means, thus concluding that among the two there is no relevant change in the response. As far as the time, all of the terms share similar means, therefore, all values can have identical responses. Main effect plot in Figure 13 shows that the

Figure 12 FX256 – Strain at break main effects and interactions plots

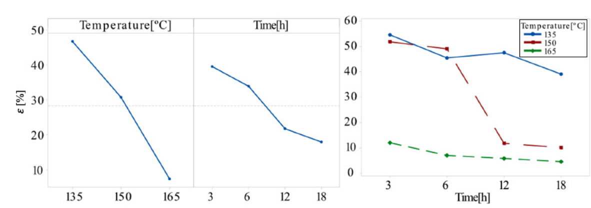

Figure 13 FX256 – Flexural modulus main effects and interactions plots

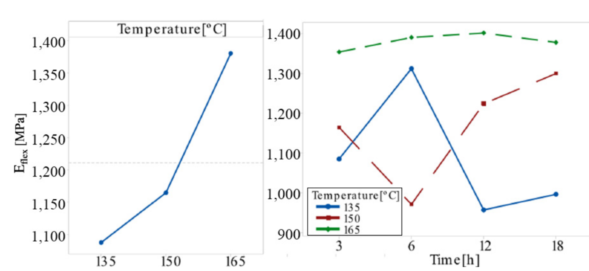

best behaviour is found at higher temperatures, regardless of the annealing time. Considering that t input variables do present evidences to deny the null hypotheses, the variation through time is difficult to evaluate without more complex statistical analysis (e.g Scott knot).

Considering flexural strength, ANOVA results indicate T [$F(2,48) = 57.28$, $p < 0.001$], which contributes 38.68%, while t [$F(3,48) = 10.77$, $p < 0.001$] with a contribution of 10.91%, whereas the interaction T-t [$F(6,48) = 16.88$, $p < 0.001$] presents a contribution of 34.20%. Post hoc Fisher comparison indicates that the three temperature stages present distinct means which translates into three different responses having to be considered. Time comparisons indicates that t = 3h presents distinct mean from all of the specimens, while 6 and 12 h share similar means, as well as 12 and 18 h, implying that only t = 3h shows a relevant change in the response. Taking into consideration the main effect plots (Figure 14), it is perceived that the best flexural strength is achieved for 150°C/3 h. The interaction plot shows a steady response along the time for T = 150°C. However, T = 135°C presents an increase in strength at t = 6 h and a consequent drop, while T = 165°C presents an overall decrease in flexural strength as the time progresses.

ANOVA results for flexural strain show that T [$F(2,48) = 96.51$, $p < 0.001$] with a contribution of 74.57%, while t [$F(3,48) = 3.94$, $p = 0.014$] contributing 4.56%, whereas the interaction T-t presented a p-value outside the confidence level, thus being disregarded. Comparing the values inside the group with Fisher LSD, it is possible to verify that T = 135 and 150°C present identical means, thus concluding that there is no relevant change in the response for those parameters. Comparing the time responses, it is possible to identify two different stages of results. Identical means for 3 to 6 h of treatment resulting in one stage, whereas 6, 12 and 18 h also present identical means among them. Considering Figure 15 results, maximum flexural strain is achieved for 135–150°C/3 h.

Figure 14 FX256 – Flexural strength main effects and interactions plots

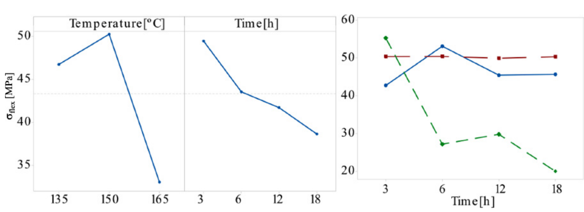

Figure 15 FX256 – Flexural strain main effects and interactions plots

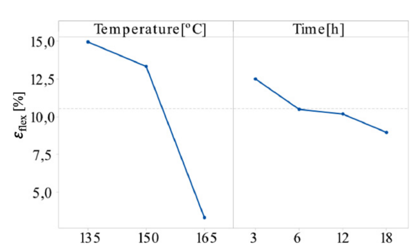

3.5 Discussion

Table 6 presents an overview of the results obtained through the statistical analysis, in which the best T/t interval is selected accordingly to the property. Through this table, it is possible to observe that t = 3 h interval is common to both materials' flexural and tensile responses with statistically significant results, indicating that t = 3 h is the ideal annealing time for an overall property increase. Considering annealing temperature, both materials' tensile and flexural properties apart from the modulus and σ_{flex}, present the common value of T = 135°C for improved properties.

Table 7 depicts the property results in agreement with the statistical analysis. For the properties which ANOVA and post hoc did not present any convergent solution, a maximized combination was selected, presenting the condition number (C) correspondent to the full factorial experience (Table 4). To summarize the results, improvement percentage for each property is also presented. It is also shown that, for the best conditions, the improvements were significantly higher for the unreinforced material, apart from the strain at break. In terms of flexural results, the improvement was also considerably higher for FX256, even though CF15 presented superior maximum values of flexural stress and modulus after treatment. Considering that both materials showed increase in flexural strain, it is possible that beyond the morphological alterations, the annealing process could promote a better interlayer behaviour.

Throughout the printing process, it became clear that the unreinforced material was more complex to print. This was corroborated by the DSC tests of the control specimens, in which higher crystallinity percentage was present in FX256, thus justifying the higher contraction levels during production. The results presented in Table 5 indicate that the increase in annealing temperatures, allied to slower cooling rates, lead to an increase in crystallinity (more accentuated in the unreinforced material) as shown in literature (Fischer and Drummer, 2016). It is also perceived that higher crystallinity levels lead to increased brittleness, justifying the decrease in strain along the defined conditions.

A decrease in performance was also found throughout the testing experiment matrix. Considering tensile strength results, it is possible to observe that FX256 performance starts to decay from C7 (in which higher change in colour is observable) onwards, while CF15 tensile strength kept higher than the control C0 until C10. As for the flexural strength, both presented decrease in performance after C10 being FX256, the most negatively influenced by the annealing condition. This decrease in properties may be also an indicative that thermal degradation of the polymer occurred at higher temperatures, most notoriously for higher treatment time periods indicating polymeric ageing possibility. A similar scenario was observed for the strain results, which allied to the increase in crystallinity might have originated the brittle behaviour.

4. Conclusion

In this work, a full factorial DOE and statistical analyses were made to identify how PA12 and reinforced PA12 printed specimens react to a wide range of temperatures and time conditions, considering mechanical behaviour as the response.

Table 6 Best annealing conditions according ANOVA's analysis

	Tensile			Flexural		
Material	Property	Temperature (°C)	Time (h)	Property	Temperature (°C)	Time (h)
CF15	E [MPa]	165	–	E_{flex} [MPa]	–	–
	σ [MPa]	135–150	3–6	σ_{flex} [MPa]	135–150	3
	ϵ [%]	135	3	ϵ_{flex}[%]	135	3
FX256	E [MPa]	–	–	E_{flex} [MPa]	165	–
	σ [MPa]	135	3–6	σ_{flex} [MPa]	150	3
	ϵ [%]	135	3	ϵ_{flex}[%]	135–150	3

Table 7 Mechanical properties overview

	Tensile					Flexural					
Material	C	Property	Control	Treated	↑[%]	C	Property	Control	Treated	↑[%]
CF15	12	E [MPa]	885.97 ± 11.66	979.19 ± 91.05	10.52	12	E_{flex} [MPa]	1748.48 ± 60.95	1923.06 ± 555.49	9.98
	5	σ [MPa]	40.36 ± 1.93	44.75 ± 1.87	10.88	5	σ_{flex} [MPa]	55.55 ± 1.74	61.45 ± 2.18	10.62
	1	ϵ [%]	25.04 ± 4.88	17.67 ± 2.30	−29.43	1	ϵ_{flex}[%]	13.06 ± 0.96	14.99 ± 2.79	14.78
FX256	6	E [MPa]	450.99 ± 54.02	559.81 ± 32.81	24.13	11	E_{flex} [MPa]	1114.31 ± 38.98	1400.90 ± 138.15	25.72
	2	σ [MPa]	29.49 ± 0.59	32.52 ± 1.79	10.27	6	σ_{flex} [MPa]	38.77 ± 10.21	50.36 ± 3.45	29.89
	1	ϵ [%]	61.19 ± 7.31	54.592 ± 5.52	−10.78	1	ϵ_{flex}[%]	9.40 ± 4.08	16.00 ± 1.48	70.21

This way, it was possible to define the best annealing conditions according with the type of property that is intended to maximise. Mechanical performance tests show that annealing theses materials can be in fact used as a method of increasing their mechanical properties. After thermal treatment, both materials showed similar crystallization degrees. Both materials show an increase in flexural properties for all properties studied. While CF15 improvement was from 10 to 15% for all properties, FX256 presented the bigger improvement of 26, 30 and 70% for E_{flex}, σ_{flex} and ϵ_{flex} correspondingly. Tensile tests show that the best conditions present an increase from 11% (E and σ), while the strain is reduced 29% for CF15. FX256 shows an increase of 24 and 10% (E and σ), in spite of a decrease of 10% in strain being demonstrated. Flexural results show an improvement of all the properties, indicating that the annealing treatment promotes a relief of residual thermal stresses resultant of the 3D printing process and, at the same time, an enhanced inter-layer adhesion. Therefore, it can be stated that annealing in PA12 and short fibre-reinforced PA12 printed parts leads to the improvement of their mechanical performance. In a general manner, as the mechanical properties of a polymer increase, their processing temperatures will most likely be higher. It was also found that T = 165°C is not indicated for thermally treat these two types of polymers, as a decrease in properties was found by comparison with the C0 specimen. When considering a process such as FFF, in which successive heating and cooling cycles are a part of the process, residual stresses are created, distorting the part leading to warping and other defects. Thermal annealing is a process that beyond the intended increase in properties, can largely reduce internal stresses due to its slow heating, molecular relaxation and consequent slow cooling, leading to more stable parts.

References

Abhari, R.E., Mouthuy, P.-A., Zargar, N., Brown, C. and Carr, A. (2017), "Effect of annealing on the mechanical properties and the degradation of electrospun polydioxanone filaments", *Journal of the Mechanical Behavior of Biomedical Materials*, Vol. 67, pp. 127-134.

Bai, H., Luo, F., Zhou, T., Deng, H., Wang, K. and Fu, Q. (2011), "New insight on the annealing induced microstructural changes and their roles in the toughening of β-form polypropylene", *Polymer*, Vol. 52 No. 10, pp. 2351-2360.

Blaine, R.L. (2002), "Thermal applications note – polymer heats of fusion".

Canevarolo, S.V. JR, (2002), *Ciência Dos Polímeros: um Texto Básico Para Tecnólogos e Engenheiros*, 2© edição ed., Artliber.

Carrascal, I., Casado, J.A., Polanco, J.A. and Gutiérrez-Solana, F. (2005), "Absorption and diffusion of humidity in fiberglass-reinforced polyamide", *Polymer Composites*, Vol. 26 No. 5, pp. 580-586.

Chen, Z., Li, Z., Li, J., Liu, C., Lao, C., Fu, Y., Liu, C., Li, Y., Wang, P. and He, Y. (2019), "3D printing of ceramics: a review", *Journal of the European Ceramic Society*, Vol. 39 No. 4, pp. 661-687.

Do, V.T., Nguyen-Tran, H.D. and Chun, D.M. (2015), "Effect of polypropylene on the mechanical properties and water absorption of carbon-fiber-reinforced-polyamide-6/polypropylene composite", *Composite Structures*, Vol. 150, pp. 240-245.

Dong, J., Mei, C., Han, J., Lee, S. and Wu, Q. (2019), "3D printed poly(lactic acid) composites with grafted cellulose nanofibers: effect of nanofiber and post-fabrication annealing treatment on composite flexural properties", *Additive Manufacturing*, Vol. 28, pp. 621-628.

Fan, W., Li, J.L., Zheng, Y.Y., Liu, T.J., Tian, X. and Sun, R.J. (2016), "Influence of thermo-oxidative aging on the thermal conductivity of carbon fiber fabric reinforced epoxy composites", *Polymer Degradation and Stability*, Vol. 123, pp. 162-169.

Fischer, E.W. (1972), "Effect of annealing and temperature on the morphological structure of polymers", *Pure and Applied Chemistry*, Vol. 31 Nos 1/2, pp. 113-131.

Fischer, C. and Drummer, D. (2016), "Crystallization and mechanical properties of polypropylene under processing-relevant cooling conditions with respect to isothermal holding time", *International Journal of Polymer Science*, Vol. 2016.

Fonseca, J., Ferreira, I.A., De Moura, M.F.S.F., Machado, M. and Alves, J.L. (2019), "Study of the interlaminar fracture under mode I loading on FFF printed parts", *Composite Structures*, Vol. 214, pp. 316-324.

García-Moreno, I., Ángel Caminero, M., Patricia Rodríguez, G. and José López-Cela, J. (2019), "Effect of thermal ageing on the impact and flexural damage behaviour of carbon fibre-reinforced epoxy laminates", *Polymers*, Vol. 11 No. 1, p. 80.

Gibson, M.A., Mykulowycz, N.M., Shim, J., Fontana, R., Schmitt, P., Roberts, A., Ketkaew, J., Shao, L., Chen, W., Bordeenithikasem, P. and Myerberg, J.S. (2018), "3D printing metals like thermoplastics: fused filament fabrication of metallic glasses", *Materials Today*, Vol. 21 No. 7, pp. 697-702.

Gogolewski, S., Czerntawska, K. and Gastorek, M. (1980), "Effect of annealing on thermal properties and crystalline structure of polyamides. Nylon 12 (polylaurolactam)", *Colloid and Polymer Science*, Vol. 258 No. 10, pp. 1130-1136.

Hart, K.R., Dunn, R.M., Sietins, J.M., Hofmeister Mock, C.M., Mackay, M.E. and Wetzel, E.D. (2018), "Increased fracture toughness of additively manufactured amorphous thermoplastics via thermal annealing", *Polymer*, Vol. 144, pp. 192-204.

International Standards Organization (2010), "ISO 178: 2010 – plastics – determination of flexural properties".

International Standards Organization (2012), "ISO 527-2:2012 – plastics – determination of tensile properties".

ISO/ASTM 52900 (2015), Standard terminology for additive manufacturing technologies – general principles – terminology.

Liu, Z., Lei, Q. and Xing, S. (2019), "Mechanical characteristics of wood, ceramic, metal and carbon fiber-based PLA composites fabricated by FDM", *Journal of Materials Research and Technology*, Vol. 8 No. 5, pp. 3741-3751.

Parzlich s.r.o. Fillamentum (2018), "Nylon FX256 material datasheet", access date: 2018-05-28.

Parzlich s.r.o. Fillamentum (2019), "Nylon CF15 carbon material datasheet", access date: 2019-05-28.

Rajeesh, K.R., Gnanamoorthy, R. and Velmurugan, R. (2010), "Effect of humidity on the indentation hardness and flexural fatigue behavior of polyamide 6 nanocomposite", *Materials Science and Engineering: A*, Vol. 527 No. 12, pp. 2826-2830.

Rangisetty, S. and Peel, L.D. (2017), "The effect of infill patterns and annealing on mechanical properties of additively manufactured thermoplastic composites", *Proceedings of the ASME 2017 Conference on Smart Materials, Adaptive Structures and Intelligent Systems*, pp. 1-12.

Sang, L., Wang, C., Wang, Y. and Wei, Z. (2017), "Thermo-oxidative ageing effect on mechanical properties and morphology of short fibre reinforced polyamide composites-comparison of carbon and glass fibres", *RSC Advances*, Vol. 7 No. 69, pp. 43334-43344.

Wohlers, T. (2018), Wohlers Report 2018: Additive Manufacturing and 3D printing State of the Industry Annual Worldwide Progress Report, Wohlers Associates.

Corresponding author

Isaac Ferreira can be contacted at: isaacaferreira@gmail.com